doi: 10.1111/j.1365-3121.2008.00811.x

Do major oxide tectonic discrimination diagrams work? Evaluating new log-ratio and discriminant-analysis-based diagrams with Indian Ocean mafic volcanics and Asian ophiolites

Hetu C. Sheth

Department of Earth Sciences, Indian Institute of Technology (IIT) Bombay, Powai, Mumbai 400076, India

ABSTRACT

Many geochemical diagrams exist that classify old volcanic terranes of ambiguous provenance into various modern plate tectonic settings, with variable success. Recently proposed diagrams, based on log-ratios and linear discriminant analysis with large datasets of major oxides, were tested here with data for ocean island, arc and mid-ocean ridge lavas from the Indian Ocean. Success rates are 45–100%, with misclassifications potentially caused by alteration, although alteration demonstrably need not cause misclassification. The diagrams were further applied to some Asian ophiolites, representing Tethyan and Indian ocean crusts, to see if the diagrams confirm their tectonic setting inferred from trace and isotopic data. Lower success rates (30–60%, but 75–100% for specific suites) are not surprising in view of the ubiquitous and complex alteration in ophiolites. Log-ratio transformation and linear discriminant analysis appear to be powerful methods when discrimination diagrams are based on major oxide data alone.

Terra Nova, 20, 229–236, 2008

Introduction

Over the years several igneous geochemists have devised geochemical diagrams that discriminate between volcanic rocks of various plate tectonic settings and which might reveal the original tectonic setting of volcanic terranes that have been transported, deformed and metamorphosed. Early schemes were based on the relatively small datasets on volcanic rocks available then (a few hundred samples) and the boundaries between the various fields were constructed by the eye, and thus subjective (e.g. Pearce and Cann, 1971, 1973). Agrawal (1999) showed the use of probability-based classifier surfaces as boundaries between rock categories, and Agrawal *et al.* (2004) used them in major oxide plots based on linear discriminant analysis of >1000 samples of volcanics from various tectonic settings. In sync with a fast-growing global database of volcanic rock compositions, there is a current surge of interest and activity in this field, and very recent literature includes extensive evaluations of existing schemes (e.g. Snow, 2006; Vermeesch, 2006a) as well as new ingenious schemes (e.g. Shragge and Snow, 2006; Vermeesch, 2000b; Verma *et al.*, 2006). In this study, I evaluated the discriminating power of diagrams proposed by Verma *et al.* (2006) (called VGA06 hereafter) and Vermeesch (2006a) (V06a hereafter).

Correspondence: H. C. Sheth, Department of Earth Sciences, Indian Institute of Technology (IIT) Bombay, Powai, Mumbai 400076, India. Tel.: +91 22 25767264; fax: +91 22 25767253; e-mail: hcsheth@iitb.ac.in

The diagrams, test data and data processing

The VGA06 diagrams (Fig. 2) are based on a large training set (2300 samples) of young (Late Miocene through Recent) basic ($SiO_2 < 52$ wt.%) and some ultrabasic rocks ($SiO_2 < 45$ wt.%) from four tectonic settings (ocean island, island arc, mid-ocean ridge and continental rift). With 400 additional (test) samples, they yielded successful classification rates of 83–97%. The V06a plot (Fig. 3) is based on 738 training samples with SiO_2 values between 45% and 53% belonging to OIB, IAB and MORB categories.

Rollinson (1993) has asked whether geochemical diagrams fundamentally *can* indicate tectonic setting because igneous rock compositions are strongly determined by sources (mantle and crustal) and processes (partial melting, fractionation, contamination) and not directly by tectonic setting. Continental crustal contamination, not a consideration for oceanic volcanics, can be significant for continental rift basalts. The 52% SiO_2 cutoff used by VGA06 does not imply that such rocks are free of crustal contamination (indeed the converse may be true, as more primitive, hotter liquids may assimilate much more crust than evolved liquids, e.g. Huppert and Sparks, 1985). However, basic and ultrabasic rocks would have a vastly larger mantle input than evolved rocks, which may even be continental crustal melts (e.g. Verma, 2000).

Major oxide data in an analysis must add to 100% and are thus subject to closure, and spurious correlations exist in such closed datasets (Chayes, 1960). Aitchison (1982, 1986) proposed log-ratio transformation to 'free' the data values to range from $-\infty$ to $+\infty$, and both VGA06 and V06a take advantage of this desirable property. Both use SiO_2 (the most abundant oxide) as the denominator to all ratios, and have performed linear discriminant analysis of the log-ratio data to obtain two discriminant functions. The V06a plot is a modification of one by Pearce (1976), who performed linear discriminant analysis but was unaware of closure (Vermeesch, 2006a). The differences between the VGA06 and V06a diagrams are that whereas the former contain discriminant functions including all the oxides, the latter's functions exclude FeO, Fe_2O_3 and P_2O_5. Due conversion of total Fe into Fe^{2+} and Fe^{3+} is an important step in the VGA06 diagrams, for which the proposal of Middlemost (1989) is used. The field boundaries are probability-based surfaces (Agrawal, 1999). LOI-free major oxide data are obtained using the SINCLAS program of Verma *et al.* (2002).

The VGA06 diagrams are five diagrams, offering all possible combinations of the OIB-CRB-MORB-IAB groups. I tested the VGA06 and V06a diagrams here using 333 samples of mafic volcanics from the Indian Ocean region (Fig. 1). The data come from the archetypal ocean islands of Mauritius and Rodrigues (110 and 10 samples, respectively), the arc volcano Barren Island in the Andaman Sea (45 samples), and the Carlsberg and Southwest Indian ridges (40 and 128 samples respectively). I then applied the diagrams to ophiolites (96 samples) in Iran, Pakistan, Tibet and the Andaman islands that represent remnants of the Tethyan and Indian oceanic crusts. None of these samples is among the >2700 total samples used by VGA06, or the $\sim$1000 samples used by V06a, in their training and testing sets.

The results

Figure 4 is the total alkalis-silica (TAS) diagram (Le Bas *et al.*, 1986) showing the general characteristics of the test samples. Almost all Mauritius and Rodrigues samples are basic, and a few ultrabasic, and most of these alkalic. Several Barren Island samples are basaltic andesite, and two andesite. The Carlsberg Ridge sample suite does not resemble typical N-MORB (which are low-K tholeiites), but are rather alkalic. Most Southwest Indian Ridge samples are true N-MORB. Figures 2 and 3 show the data for them on the VGA06 and V06a diagrams, and Tables 1 and 2 give the number of samples that lie within a particular field in each, along with the overall percentage success rates for each rock suite. The main observations and interpretations follow.

Mauritius and Rodrigues OIB

The raw and adjusted (LOI-free) SiO_2 values are all ≤52%. However, the VGA06 diagrams classify almost 60% of the Mauritius samples with CRB, with only 37% with OIB, and 80% of

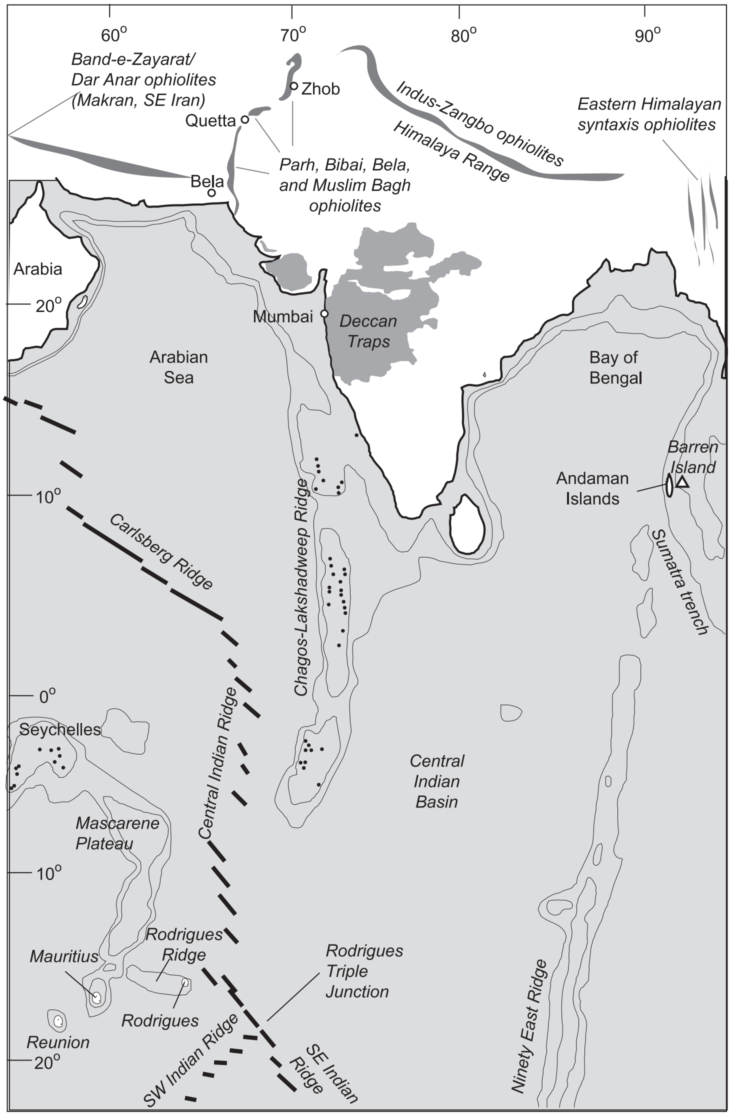

Fig. 1 Map of the main geographical and geological features of the Indian Ocean and bordering landmasses. Modified from Mahoney *et al.* (2002a,b) and Zhang *et al.* (2005).

the Rodrigues samples with OIB. This means that OIB and CRB cannot be distinguished by VGA06, something these authors found with their own testing set. There are strong chemical and isotopic similarities between CRB and OIB (e.g. Smith, 1993; Fitton, 2007). OIB-like magmas are abundant in continental rifts, suggesting closely similar mantle sources. Although mantle plumes are often invoked for both OIB and CRB, OIB-type chemistry is no longer considered diagnostic of plumes (Natland and Winterer, 2005; Hofmann and Hart, 2005; Fitton, 2007). CRB and OIB also cannot be distinguished with *alteration-resistant trace elements* such as Nb and Zr (Fitton, 2007).

The V06a plot correctly classifies 77% of the Mauritius (but only 60% of the Rodrigues) samples, partly because of its different discriminant functions. But it has also an edge over VGA06 by *not having* a CRB category to which OIBs can be so similar. Indeed, dropping the CRB category dramatically improves the performance of the VGA06 diagrams (Table 3). Whereas the VGA06 diagrams together perform much more poorly than the V06a plot, the VGA06

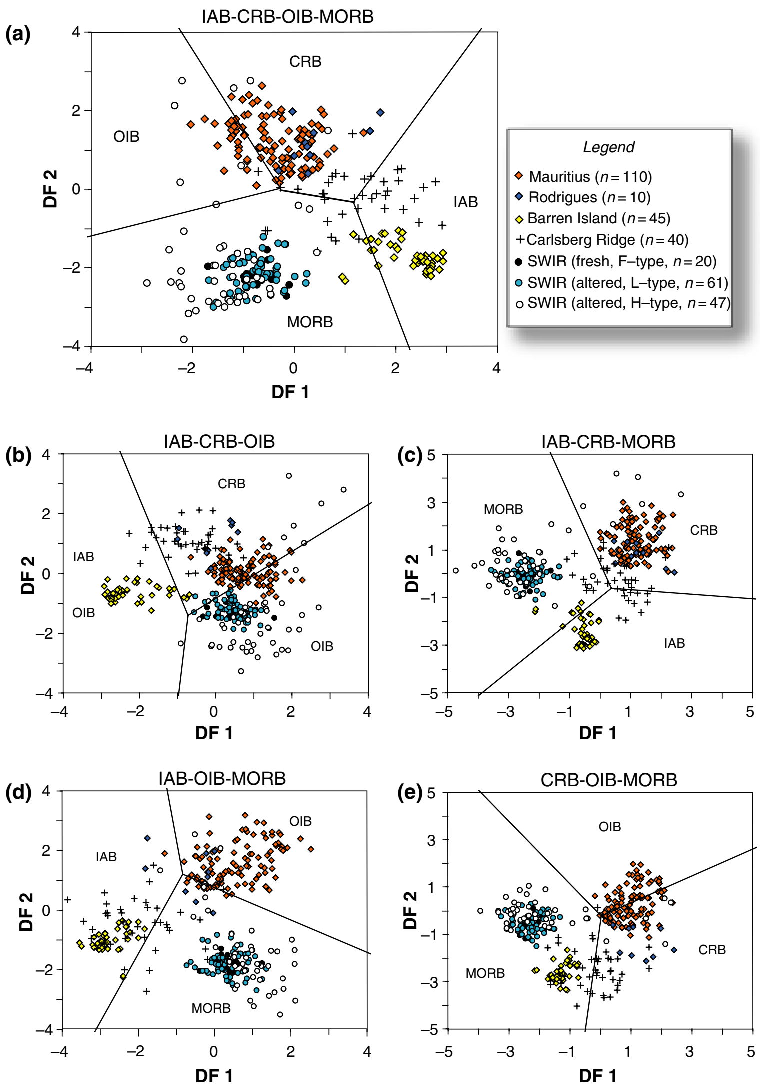

Fig. 2 (a–e) Data for Indian Ocean volcanics on the discrimination diagrams of Verma *et al.* (2006). The linear equations for discriminant functions DF1 and DF2 for each of the five plots can be found in Verma *et al.* (2006). Data sources are: Mauritius Older, Intermediate and Younger Series (Sheth *et al.*, 2003; Nohda *et al.*, 2005; Paul *et al.*, 2005, 2007); Mauritius Older Differentiated Series (Paul *et al.*, 2007); Rodrigues (Baxter *et al.*, 1985); Barren Island (Alam *et al.*, 2004; Luhr and Haldar, 2006; Pal *et al.*, 2007); Carlsberg Ridge MORB (Banerjee and Iyer, 1991); Southwest Indian Ridge MORB (Nakamura *et al.*, 2007).

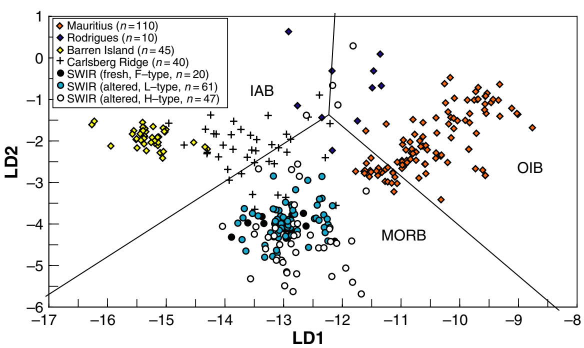

Fig. 3 Data for the suites shown in Fig. 2, on the Vermeesch (2006a) plot.

'd' diagram, without a CRB category, has a much better individual performance, comparable to that of V06a (Table 3). Thus, more categories in such diagrams do not mean improved performance; rather, the opposite can be true. Finally, because an overwhelming majority of ophiolite suites are oceanic (and few, if any, CRB suites would become ophiolites), it may be worthwhile to drop the CRB category from such diagrams.

Barren Island arc volcano

Several of the 45 samples notably have LOI-free SiO_2 > 52%, the upper limit for the VGA06 diagrams, and therefore these should strictly not be tested. Nevertheless, these diagrams show an overall (and minimum) success rate of 72%, and seem to work well for arc rocks. The V06a plot correctly classifies 100% of these, indicating that the degree of differentiation is not a concern over this SiO_2 range.

Carlsberg Ridge

Not too surprisingly, most Carlsberg Ridge MORB samples are not classified with MORB in the five VGA06 diagrams. In fact, overall 72% of these samples are classified as IAB and 26% as MORB. On the V06a plot, only 37.5% of these samples are classified with MORB, and 67.5% are misclassified with OIB. It was noted from the TAS diagram (Fig. 4) that these rocks are not N-MORB. They may be enriched (E)-MORB. E-MORB are abundant along a very long section of the Southeast Indian Ridge east of ~100°E, without any nearby hotspot (Mahoney *et al.*, 2002a). Trace element data for the Carlsberg Ridge suite here (Banerjee and Iyer, 1991) are limited to Ni, Co, Cr and Cu, and hence the possible E-MORB nature of this suite cannot be ascertained. Part of the problem may be that several major oxides in this study were measured by atomic absorption spectrophotometry, where instrumental calibration with mono-element solutions (as opposed to the multielement natural rocks) is the norm. Alternatively, the alkalic compositions of this suite (and their misclassification in the diagrams) may be because of weathering and alteration (see e.g. Verma, 1981; Jochum and

Table 1 Percentage classifications for volcanic rocks from the Mauritius and Rodrigues ocean islands, Barren Island arc volcano, and Carlsberg and Southwest Indian Ridges on the Verma *et al.* (2006) diagrams.

Fig. no.	OIB (n) 2a	2b	2c	2d	2e	CRB (n) 2a	2b	2c	2d	2e	MORB (n) 2a	2b	2c	2d	2e	IAB (n) 2a	2b	2c	2d	2e	OIB (%)	CRB (%)	MORB (%)	IAB (%)
Maur (n = 110)	21	25	–	94	64	89	85	110	–	45	0	–	0	15	1	0	0	0	1	–	204/550 (37.1)	329/550 (**59.8**)	16/550 (2.91)	1/550 (0.002)
Rodr (n = 10)	0	0	–	4	0	10	10	10	–	10	0	–	0	4	0	0	0	0	2	–	4/50 (8.00)	40/50 (**80.0**)	4/50 (8.00)	2/50 (4.00)
Barren (n = 45)	0	0	–	0	0	0	3	0	–	0	6	–	8	0	45	39	42	37	45	–	0/225 (0.00)	3/225 (1.33)	59/225 (26.2)	163/225 (**72.4**)
Carls (n = 40)	1	0	–	1	1	12	35	19	–	24	10	–	9	11	15	17	5	12	28	–	3/200 (1.50)	90/200 (45.0)	45/200 (22.5)	62/200 (31.0)
SWIR F-type (n = 20)	0	20	–	0	0	0	0	0	–	0	20	–	20	20	20	0	0	0	0	–	20/100 (20.0)	0/100 (0.00)	80/100 (**80.0**)	0/100 (0.00)
SWIR L-type (n = 61)	0	57	–	0	0	0	4	0	–	0	61	–	61	61	61	0	0	0	0	–	57/305 (18.7)	4/305 (1.31)	244/305 (**80.0**)	0/305 (0.00)
SWIR H-type (n = 47)	4	38	–	2	0	2	8	6	–	5	41	–	41	44	42	0	1	0	1	–	44/235 (18.7)	21/235 (8.94)	168/235 (**71.5**)	2/235 (0.85)
SWIR overall (n = 128)	4	115	–	2	0	2	12	6	–	5	122	–	122	125	123	0	1	0	1	–	121/640 (18.9)	25/640 (3.91)	492/640 (**76.9**)	2/640 (0.31)

The data are arranged to show the number of samples of a particular rock suite that lie within a specific field (tectonic setting) in each of the diagrams. For example, the number of samples of Mauritius rocks (110 in total) that lie within the fields of OIB, CRB, MORB and IAB are 21, 89, 0 and 0 respectively (see the '2a' columns under all four categories). The percentage of samples that lies within each of the four fields is calculated as the sum of values in any category divided by five times the number of total samples for that rock suite, multiplied by 100. For example, the number of Mauritius rock samples classified as OIB, in diagrams 2a through 2e, is (21 + 25 + 94 + 64) = 204. This, divided by 550 (the total number of 'tries', 110 × 5), and multiplied by 100 gives the percentage of Mauritius samples classified as OIB as 37.1. Zeros in a particular cell mean that the particular tectonic field was available in a plot but no samples plotted in it, whereas dashes mean that the particular tectonic field was not present in the plot. Because Fig. 2b–d successively exclude each of the four tectonic fields, any biases and wrong assignments to sample points because of the 'correct' field simply not being available in a plot should mutually cancel out. Percentages close to and above 50% are shown in boldface. F-type SWIR MORB are fresh MORB, L-type are low-degree weathered MORB, and H-type are high-degree weathered MORB (see text).

Verma, 1996). However, Banerjee and Iyer (1991) did not notice the samples to be particularly altered, and in the case of the next rock suite, demonstrable weathering and alteration *have not caused* a significant misclassification.

Southwest Indian Ridge MORB

The study by Nakamura *et al.* (2007) offers an opportunity to apply the VGA06 and V06a diagrams to fresh and altered MORB from the same area, and thus to evaluate the role of weathering and alteration in misclassification. Their 128 samples come from the Southwest Indian Ridge, near the Rodrigues Triple Junction. On the basis of petrographic (celadonite, chlorite, etc.) and geochemical evidence, they have divided the rocks into fresh (20 samples), low-temperature altered (61 samples), and high-temperature, hydrothermally altered (47 samples).

Eighty per cent of the fresh SWIR MORB samples are classified with the MORB category in the VGA06 diagrams, and all 100% in the V06a plot. What is remarkable, however, is that these results and results for low-temperature and high-temperature altered MORB are closely similar. The VGA06 and V06a diagrams correctly classify 80% and 100%, respectively, of the low-temperature altered MORB. For the high-temperature altered MORB, the success rates are lower with the VGA06 diagrams (71.5%), but as high as 91.5% with the V06a plot. Considering the SWIR MORB suite as a whole, the success rate with the VGA06 diagrams is 76.9, and with the V06a plot it is as high as 96.9. This is consistent with VGA06 who reported the highest success rates (as high as 97%) with MORB. This is proof that whereas specific types of alteration may cause misclassification in particular cases, alteration does not always cause misclassification – a highly encouraging result.

Case study: Asian ophiolites

Ophiolites are almost always structurally deformed and altered, if not metamorphosed as well. Many ophiolite suites that outcrop in Asia represent long-subducted Tethyan and Indian oceanic crusts. Because the tectonic setting of several is well

Table 2 Classification percentages for volcanic rocks from the Mauritius and Rodrigues ocean islands, Barren Island arc volcano, and Carlsberg and Southwest Indian Ridges with the Vermeesch (2006a) diagram.

	OIB (*n*)	MORB (*n*)	IAB (*n*)	OIB (%)	MORB (%)	IAB (%)
Fig. no. 3						
Mauritius (*n* = 110)	85	25	0	**77.3**	22.7	0.00
Rodrigues (*n* = 10)	6	1	3	**60.0**	10.0	30.0
Barren Is. (*n* = 45)	0	0	45	0.00	0.00	**100**
Carlsberg Ridge (*n* = 40)	25	15	0	**62.5**	37.5	0.00
SWIR, F-type (*n* = 20)	0	20	0	0.00	**100**	0.00
SWIR, L-type (*n* = 61)	0	61	0	0.00	**100**	0.00
SWIR, H-type (*n* = 47)	3	43	1	6.38	**91.5**	2.13
SWIR, overall (*n* = 128)	3	124	1	2.34	**96.9**	0.78

Table 3 Side-by-side comparison of the number of correctly classified modern oceanic basalts using the VGA06 (all five), VGA06 (only 'd'), and V06a diagrams.

Locality	VGA06, all five	V06a	VGA06, 'd' only
Mauritius (OIB)	37.1% (=204/550)	77.3% (=85/110)	85.4% (=94/110)
Rodrigues (OIB)	8.00% (=4/50)	60.0% (=6/10)	40.0% (=4/10)
Barren Is. (IAB)	72.4% (=163/225)	100% (=45/45)	100% (=45/45)
Carlsberg R. (MORB)	22.5% (=45/200)	37.5% (=15/40)	27.5% (=11/40)
SWIR, F-type (MORB)	80.0% (=80/100)	100% (=20/20)	100% (=20/20)
SWIR, L-type (MORB)	80.0% (=244/305)	100% (=61/61)	100% (=61/61)
SWIR, H-type (MORB)	71.5% (=168/235)	91.5% (=43/47)	93.6% (=44/47)
SWIR, MORB overall	76.9% (=492/640)	96.9 (=124/128)	97.6% (=125/128)

understood, with major and trace element and sometimes Sr-Nd-Pb isotopic determinations, it is tempting to use the current diagrams to see if these can corroborate (and presumably, by themselves reliably indicate) the setting. Figure 5 shows the data for these ophiolites on the Zr–Ti diagram, proposed by Pearce and Cann (1973) and here in its modified form after linear discriminant analysis (Vermeesch, 2006a). Some show affinities with a single tectonic category (e.g. Parh Group with OIB), and others with more than one.

Figures 6 and 7 show the data for these ophiolites on the VGA06 and V06a diagrams, and Tables 4 and 5 summarize the results. The *c.* 75 Ma Parh Group (Bibai Volcanics) alkali basalts and basanites are known to have formed as intrusions in shelf-type marine limestones and other sediments, and based on their normalized multielement patterns and isotopic evidence Mahoney *et al.* (2002b) interpret them as OIBs. The data lie in the CRB and OIB fields in Fig. 5 (and OIB field in Fig. 7) and these plots reaffirm the known great geochemical closeness of CRB to OIB. The V06a plot classifies all samples correctly with OIB. Data for the Muslim Bagh ophiolite cover all fields in the VGA06 diagrams with the MORB field slightly dominating (48.6% MORB followed by 23.8% IAB samples); notably, these were interpreted as of composite tectonic setting (ridge plus arc) based on trace element and other evidence (Khan *et al.*, 2007). They are indeed classified as MORB (52%) and IAB (38%) by the V06a plot, and straddle across all the fields in Fig. 7. The Band-e-Zeyarat/Dar Anar ophiolite of Makran was interpreted as MORB based on elemental and Sr-Nd-Pb isotopic evidence (Ghazi *et al.*, 2004); Table 4 shows 51% of the samples classified as MORB followed by 30% IAB samples, whereas the V06a plot classifies 55% of them with IAB. Here these diagrams perform poorly.

Sr-Nd-Pb isotopic character of the Indus-Zangbo and Eastern Himalayan syntaxis ophiolites indicates their Tethyan MORB provenance (Zhang *et al.*, 2005). 60% samples of both suites are classified as MORB with the VGA06 diagrams, and 65% and 75% respectively with the V06a plot. Finally, the South Andaman ophiolitic basalts do not show a clear preference for any field with either the VGA06 or V06a diagrams, although Srivastava *et al.* (2004) identified them with MORB with the earlier discrimination diagrams of Agrawal *et al.* (2004). The performance of the diagrams for ophiolite suites is therefore quite vari-

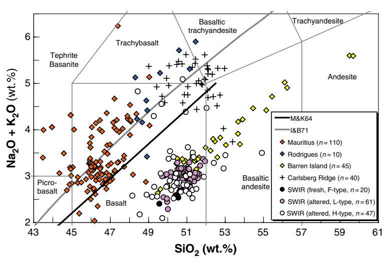

Fig. 4 TAS diagram (Le Bas *et al.*, 1986) showing the data for the suites shown in Figs 2 and 3. M&K64 and I&B71 are the boundaries between the sub-alkalic and alkalic fields by Macdonald and Katsura (1964) and Irvine and Baragar (1971).

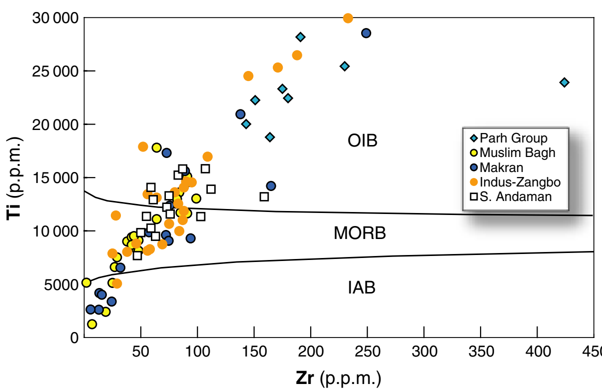

Fig. 5 Data for Tethyan and Indian oceanic crustal ophiolites on the modified Zr–Ti diagram (Vermeesch, 2006a).

Table 4 Classification percentages for the Tethyan and Indian oceanic crustal ophiolites with the Verma *et al.* (2006) diagrams.

Fig. no. 6	OIB (*n*)					CRB (*n*)					MORB (*n*)					IAB (*n*)					OIB (%)	CRB (%)	MORB (%)	IAB (%)
	6a	6b	6c	6d	6e	6a	6b	6c	6d	6e	6a	6b	6c	6d	6e	6a	6b	6c	6d	6e				
Parh group (*n* = 9)	2	4	–	9	7	7	5	9	–	2	0	–	0	0	0	0	0	0	0	–	22/45 (**48.9**)	23/45 (**51.1**)	0/45 (0.00)	0/45 (0.00)
Muslim Bagh (*n* = 21)	0	6	–	6	5	1	7	0	–	4	14	–	16	9	12	6	8	5	6	–	17/105 (16.2)	12/105 (11.4)	51/105 (**48.6**)	25/105 (23.8)
Makran (*n* = 18)	2	5	–	1	1	1	5	1	–	1	9	–	11	10	16	6	8	6	7	–	9/90 (10.0)	8/90 (8.89)	46/90 (**51.1**)	27/90 (30.0)
Indus-Zangbo (*n* = 26)	5	15	–	3	3	1	6	2	–	2	17	–	21	20	21	3	5	3	3	–	26/130 (20.0)	11/130 (8.46)	79/130 (**60.8**)	14/130 (10.8)
E. Himalayas syntaxis (*n* = 4)	0	1	–	0	0	0	1	0	–	1	3	–	3	3	3	1	2	1	1	–	1/20 (5.00)	2/20 (10.0)	12/20 (**60.0**)	5/20 (25.0)
S. Andaman (*n* = 16)	0	2	–	1	1	4	9	5	–	8	7	–	6	6	7	5	5	5	9	–	4/80 (5.00)	26/80 (32.5)	26/80 (32.5)	24/80 (30.0)

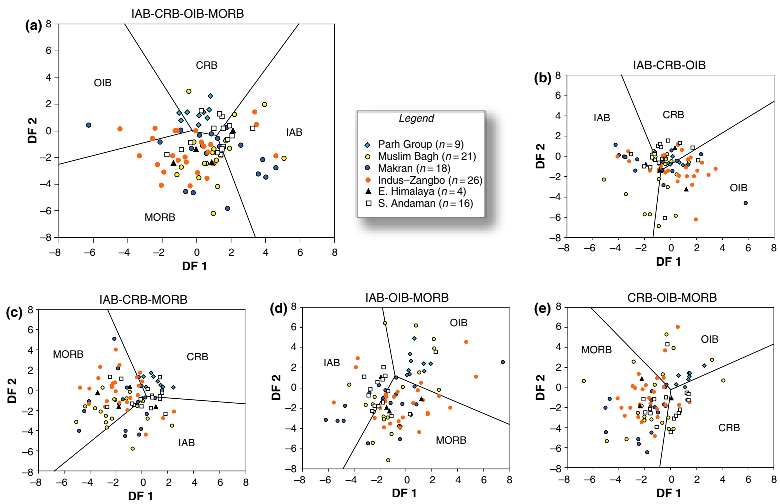

Fig. 6 (a–e) Data for Tethyan and Indian oceanic crustal ophiolites on the discrimination diagrams of Verma *et al.* (2006). Data sources are: Parh Group/Bibai volcanics (Mahoney *et al.*, 1998, 2002b); Muslim Bagh (Khan *et al.*, 2007); Band-e-Zeyarat/Dar Anar (Makran, SE Iran) (Ghazi *et al.*, 2004); Indus-Zangbo and Eastern Himalayan syntaxis (Mo *et al.*, 1994, 1998, 2005; Shen *et al.*, 2002; Zhang *et al.*, 2005); South Andaman (Srivastava *et al.*, 2004). Data for Bela ophiolite of Pakistan (interpreted as formed along a leaky transform, Sarwar, 1992) and several South Andaman samples (Srivastava *et al.*, 2004) could not be processed because of lack of P_2O_5 values.

able. It is 'very good', with 50–50% OIB + CRB or 100% OIB for the Parh Group, through 'fair', with 60–75% MORB for the Indus-Zangbo and Eastern Himalayan suites, to 'poor' for the Makran and South Andaman suites. Thus these diagrams cannot substitute for trace element and isotopic analyses, which are required and of unquestionable value. Similarly constructed diagrams of only the alteration-resistant major (Ti) and trace (e.g. Nb, Zr, Y) elements should provide still better results.

Conclusions and recommendations

Log-ratio transformation and linear discriminant analysis of large datasets in the VGA06 and V06a diagrams resolve quite well the otherwise subtle major oxide differences between mafic rocks of various tectonic categories, here selected from the Indian Ocean region. The diagrams are quite powerful with OIB, IAB and MORB. The VGA06 diagrams cannot distinguish between CRB and OIB in many cases (though no other existing scheme does). The CRB category may perhaps be dropped from future versions. However, the diagrams have a very variable performance when applied to Tethyan and Indian Ocean ophiolite suites outcropping in Asia, and as clues to the original tectonic setting of ophiolites, these remain quite inferior to trace element and isotopic data.

Table 5 Classification percentages for the Tethyan and Indian oceanic crustal ophiolites with the Vermeesch (2006a) diagram.

	OIB (*n*)	MORB (*n*)	IAB (*n*)	OIB (%)	MORB (%)	IAB (%)
Fig. no. 7						
Parh group (*n* = 9)	9	0	0	**100**	0.00	0.00
Muslim Bagh (*n* = 21)	2	11	8	9.52	**52.4**	38.1
Bela (*n* = 24)	9	13	2	37.5	**54.2**	8.33
Makran (*n* = 18)	2	6	10	11.1	33.3	**55.5**
Indus-Zangbo (*n* = 26)	4	17	5	15.4	**65.4**	19.2
E. Himalaya syntaxis (*n* = 4)	0	3	1	0.00	**75.0**	25.0
S. Andaman (*n* = 16)	1	8	7	6.25	**50.0**	43.7

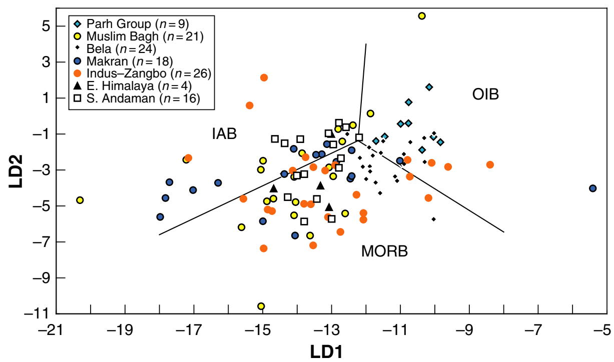

Fig. 7 The ophiolite data on the Vermeesch (2006a) plot. The Bela ophiolite, missing from Fig. 6 and Table 4, appears here because Vermeesch's (2006a) functions exclude P_2O_5.

Future geochemical schemes might employ large datasets of only the alteration-resistant major (Ti) and trace (e.g. Nb, Zr, Y) elements to acquire maximum possible power and utility (e.g. Vermeesch, 2006a,b).

Acknowledgements

I thank Surendra Pal Verma, Pieter Vermeesch, Salil Agrawal, and Mirna Guevara for papers, discussions, comments, and advice. Thorough, critical, constructive reviews of three previous versions of this manuscript by Cameron Snow and Pieter Vermeesch and editorial comments from Alfred Kröner and Gerhard Wörner are greatly appreciated.

References

Agrawal, S., 1999. Geochemical discrimination diagrams: a simple way of replacing eye-fitted boundaries with probability-based classifier surfaces. *J. Geol. Soc. Ind.*, **54**, 335–346.

Agrawal, S., Guevara, M. and Verma, S.P., 2004. Discriminant analysis applied to establish major-element field boundaries for tectonic varieties of basic rocks. *Int. Geol. Rev.*, **46**, 575–594.

Aitchison, J., 1982. The statistical analysis of compositional data. *J. Royal Stat. Soc.*, **44**, 139–177.

Aitchison, J., 1986. The statistical analysis of compositional data. Chapman and Hall, London, 416p.

Alam, M.A., Chandrasekharam, D., Vaselli, O., Capaccioni, B., Manetti, P. and Santo, P.B., 2004. Petrology of the pre-historic lavas and dyke of the Barren Island, Andaman Sea, Indian Ocean. *Proc. Ind. Acad. Sci. (Earth Planet. Sci.)*, **113**, 715–722.

Banerjee, R. and Iyer, S.D., 1991. Petrography and chemistry of basalts from the Carlsberg Ridge. *J. Geol. Soc. Ind.*, **38**, 369–386.

Baxter, A.N., Upton, B.G.J. and White, W.M., 1985. Petrology and geochemistry of Rodrigues Island, Indian Ocean. *Contrib. Mineral. Petrol.*, **89**, 90–101.

Chayes, F., 1960. On correlation between variables of constant sum. *J. Geophys. Res.*, **65**, 4185–4193.

Fitton, J.G., 2007. The OIB paradox. In: *Plates, Plumes and Planetary Processes* (G.R. Foulger and D.M. Jurdy, eds), *Geol. Soc. Am. Spec. Pap.*, **430**, 387–412.

Ghazi, A.M., Hassanipak, A.A., Mahoney, J.J. and Duncan, R.A., 2004. Geochemical characteristics, ^{40}Ar-^{39}Ar ages and original tectonic setting of the Band-e-Zeyarat/Dar Anar ophiolite, Makran accretionary prism, S. E. Iran. *Tectonophys.*, **393**, 175–196.

Hofmann, A.W. and Hart, S.R., 2005. Another nail in which coffin? *Science*, **351**, 39–40.

Huppert, H.E. and Sparks, R.S.J., 1985. Cooling and contamination of mafic and ultramafic magmas during ascent through the continental crust. *Earth Planet. Sci. Lett.*, **74**, 371–386.

Irvine, T.N. and Baragar, W.R.A., 1971. A guide to the chemical classification of the common rocks. *Can. J. Earth Sci.*, **8**, 523–548.

Jochum, K.P. and Verma, S.P., 1996. Extreme enrichment of Sb, Tl and other trace elements in altered MORB. *Chem. Geol.*, **130**, 289–299.

Khan, M., Kerr, A.C. and Mahmood, K., 2007. Formation and tectonic evolution of the Cretaceous-Jurassic Muslim Bagh ophiolitic complex, Pakistan: Implications for the composite tectonic setting of ophiolites. *J. Asian Earth Sci.*, **31**, 112–127.

Le Bas, M.J., Le Maitre, R.W., Streckeisen, A. and Zanettin, B., 1986. A chemical classification of volcanic rocks based on the total alkali-silica diagram. *J. Petrol.*, **27**, 745–750.

Luhr, J.F. and Haldar, D., 2006. Barren Island volcano (NE Indian Ocean): Island arc high-alumina basalts produced by troctolite contamination. *J. Volcanol. Geotherm. Res.*, **149**, 177–212.

Macdonald, G.A. and Katsura, T., 1964. Chemical composition of Hawaiian lavas. *J. Petrol.*, **5**, 82–133.

Mahoney, J.J., Frei, R., Tejada, M.L.G., Mo, X.X., Leat, P.T. and Nägler, T.F., 1998. Tracing the Indian Ocean mantle domain through time: isotopic results from old West Indian, East Tethyan, and South Pacific seafloor. *J. Petrol.*, **39**, 1285–1306.

Mahoney, J.J., Graham, D.W., Christie, D.M., Johnson, K.T.M., Hall, L.S. and Vonderhaar, D.L., 2002a. Between a hotspot and a cold spot: isotopic variation in the Southeast Indian Ridge asthenosphere, 86°E-118°E. *J. Petrol.*, **43**, 1155–1176.

Mahoney, J.J., Duncan, R.A., Khan, W., Gnos, E. and McCormick, G.R., 2002b. Cretaceous volcanic rocks of the South Tethyan suture zone, Pakistan: implications for the Réunion hotspot and Deccan Traps. *Earth Planet. Sci. Lett.*, **203**, 295–310.

Middlemost, E.A.K., 1989. Iron oxidation ratios, norms and the classification of volcanic rocks. *Chem. Geol.*, **77**, 19–26.

Mo, X.-X., Deng, J.-F. and Lu, F.-X., 1994. Volcanism and evolution of Tethys in Sanjiang area, southwestern China. *J. Southeast Asian Earth Sci.*, **9**, 325–333.

Mo, X.-X., Shen, S.-Y., Zhu, Q.-W., Xu, T.-R., Wei, Q.-R., Tan, J., Zhang, S.-Q. and Chen, H.-L., 1998. *Volcanics – Ophiolite and Mineralization of Middle-southern Part of Sanjiang Area of Southwestern China*. Geol. Publ. House, Beijing (in Chinese with English abstract).

Mo, X.-X., Zhao, Z.-D. and Guo, T.-Y., 2005. *Mesozoic and Cenozoic Tectono-Magmatic Events in the Tibetan Plateau*. Guangdong Sci. & Tech. Press, Guangzhou (in Chinese with extended English abstract).

Nakamura, K., Kato, Y., Tamaki, K. and Ishii, T., 2007. Geochemistry of hydrothermally altered basaltic rocks from the Southwest Indian Ridge near the Rodriguez Triple Junction. *Mar. Geol.*, **239**, 125–141.

Natland, J.H. and Winterer, E.L., 2005. Fissure control on volcanic action in the Pacific. In: *Plates, Plumes and Paradigms* (G.R. Foulger, J.H. Natland, D.C. Presnall and D.L. Anderson, eds), *Geol. Soc. Am. Spec. Pap.*, **388**, 687–710.

Nohda, S., Kaneoka, I., Hanyu, T., Xu, S. and Uto, K., 2005. Systematic variation of Sr-, Nd- and Pb-isotopes with time in lavas of Mauritius, Réunion hotspot. *J. Petrol.*, **46**, 505–522.

Pal, T., Bandopadhyay, P.C., Mitra, S.K. and Raghav, S., 2007. The 2005 eruption of Barren volcano: an explosive inner arc volcanism in Andaman Sea. *J. Geol. Soc. Ind.*, **69**, 1195–1202.

Paul, D., White, W.M. and Blichert-Toft, J., 2005. Geochemistry of Mauritius and the origin of rejuvenescent volcanism on oceanic island volcanoes. *Geochem. Geophys. Geosyst.*, **6**. Doi: 10.1029/2004GC000883.

Paul, D., Kamenetsky, V.S., Hofmann, A.W. and Stracke, A., 2007. Compositional diversity among primitive lavas of Mauritius, Indian Ocean: implications for mantle sources. *J. Volcanol. Geotherm. Res.*, **164**, 76–94.

Pearce, J.A., 1976. Statistical analysis of some major element patterns in basalts. *J. Petrol.*, **17**, 15–43.

Pearce, J.A. and Cann, J.R., 1971. Ophiolite origin investigated by discriminant analysis using Ti, Zr and Y. *Earth Planet. Sci. Lett.*, **12**, 339–349.

Pearce, J.A. and Cann, J.R., 1973. Tectonic setting of basic volcanic rocks determined using trace element analyses. *Earth Planet. Sci. Lett.*, **19**, 290–300.

Rollinson, H.R., 1993. *Using Geochemical Data: Evaluation, Presentation, Interpretation*. Longman Sci. & Tech., Essex, UK, 344 p.

Sarwar, G., 1992. Tectonic setting of the Bela ophiolites, southern Pakistan. *Tectonophysics*, **207**, 359–381.

Shen, S.-Y., Feng, Q.-L., Liu, B.-P. and Mo, X.-X., 2002. Tectonomagmatic types of volcanic rocks in South Lancangjiang belt, Sanjiang region. *Min. Rocks*, **22**, 66–71.

Sheth, H.C., Mahoney, J.J. and Baxter, A.N., 2003. Geochemistry of lavas from Mauritius, Indian Ocean: mantle sources and petrogenesis. *Int. Geol. Rev.*, **45**, 780–797.

Shragge, J. and Snow, C.A., 2006. Bayesian geochemical discrimination of mafic volcanic rocks. *Am. J. Sci.*, **306**, 191–209.

Smith, A.D., 1993. The continental mantle as a source for hotspot volcanism. *Terra Nova*, **5**, 452–460.

Snow, C.A., 2006. A reevaluation of tectonic discrimination diagrams and a new probabilistic approach using large geochemical databases: Moving beyond binary and ternary plots. *J. Geophys. Res.*, **111**. Doi: 10.1029/2005JB003799.

Srivastava, R.K., Chandra, R. and Shastry, A., 2004. High-Ti type N-MORB parentage of basalts from the south Andaman ophiolite suite, India. *Proc. Ind. Acad. Sci. (Earth Planet. Sci.)*, **113**, 605–618.

Verma, S.P., 1981. Seawater alteration effects on $^{87}Sr/^{86}Sr$, K, Rb, Cs, Ba and Sr in oceanic igneous rocks. *Chem. Geol.*, **34**, 81–89.

Verma, S.P., 2000. Geochemical and Sr-Nd-Pb isotopic evidence for a combined assimilation and fractional crystallization process for volcanic rocks from the Huichapan caldera, Hidalgo, Mexico. *Lithos*, **56**, 141–164.

Verma, S.P., Torres-Alvarado, I.S. and Sotelo-Rodriguez, Z.T., 2002. SINCLAS: standard igneous norm and volcanic rock classification system. *Comput. Geosci.*, **28**, 711–715.

Verma, S.P., Guevara, M. and Agrawal, S., 2006. Discriminating four tectonic settings: Five new geochemical diagrams for basic and ultrabasic volcanic rocks based on log-ratio transformation of major-element data. *J. Earth Syst. Sci.*, **115**, 485–528.

Vermeesch, P., 2006b. Tectonic discrimination diagrams revisited. *Geochem. Geophys. Geosyst.*, **7**, Q06017. doi: 10.1029/2005GC001092.

Vermeesch, P., 2006b. Tectonic discrimination of basalts with classification trees. *Geochim. Cosmochim. Acta*, **70**, 1839–1848.

Zhang, S.-Q., Mahoney, J.J., Mo, X.X., Ghazi, A.M., Milani, L., Crawford, A.J., Guo, T.-Y. and Zhao, Z.-D., 2005. Evidence for a widespread Tethyan upper mantle with Indian-Ocean-type isotopic characteristics. *J. Petrol.*, **46**, 829–858.

Note added: The linear discriminant function equations and coordinates for the VO6a plot used here were wrongly printed in Vermeesch (2006b). The equations and values can be found at: http://pvermees.andropov.org/noble/disc/erratum.html.

Received 11 January 2008; revised version accepted 2 April 2008

